Optica Applicata, Vol. XX, No. 3, 1990

Laser-Doppler anemometer with adaptive temporal selection of the velocity vector

P. Ya. BELOUSOV, Yu. N. DUBNISTCHEV, V. G.. MELEDIN, V. A. PAVLOV

USSR Academy of Sciences, Siberian Branch Institute of Thermophysics, Novosibirsk 630090, USSR.

The paper describes a laser-Doppler anemometer with the adaptive temporal selection of the velocity vector orthogonal components. Logic switching of measuring channels corresponds to the distribution of scattering particles and dynamics of the investigated process. The method of adaptive temporal selection is featured by the high power efficiency and the lack of switching noise.

1. Introduction

Simultaneous measurement of two orthogonal components of the velocity vector is usually performed using two-channel laser anemometers with power distributed between the channels [1], [2]. These devices have, however, a drawback, i.e., the ineffectively used laser radiation power, since only less than one half of the laser source radiation falls on the optical channel measuring one velocity component. This drawback becomes especially apparent for the measurements in backscatter, when the light signal intensity decreases by three or four orders, compared with that of forward scattered light. In commercial laser-Doppler anemometers (LDA), there is usually a chromatic or frequency separation of measuring channels. Due to the dispersion of the refractive index in the investigated media the additional error appears at chromatic selection.

In scientific literature, there are descriptions of experimental LDA models with temporal selection of signals in optical channels measuring the velocity components [3]. Forced channel switching is carried out within the interval corresponding to the time required for a scattering particle to cross a probe laser beam, laser radiation remaining distributed between the optical channels one Doppler burst. The drawback of these devices is their poor measurement accuracy resulting from the switching noise. Moreover, the presence of several scattering particles in the probe optical field makes the measurements complicated.

The present work reports on a laser-Doppler anemometer developed with adaptive temporal selection of the velocity vector. Adaptive temporal selection (ATS) makes it possible to rise considerably the signal-to-noise ratio and to improve the measurement accuracy, which is most effective at selecting information on the flow velocity components using remote measurement technique operated in backscatter. The ATS method is realized by optical and electronic means. Structurally, the said devices are two-channel, with acousto-optical or electrooptical switching of mea-

suring channels. The devices are characterized by an improved measurement accuracy due to automatic matching of temporal selection of the velocity components and spatial distribution of scattering particles in a flow. Noise stability of electronic processor also contributes to the accuracy of measurements.

2. Configurations and method

An optical configuration of LDA using acousto-optical switching measuring channels is shown in Fig. 1.

The setup comprises laser 1 and the following units placed successively on the way of the laser beam: phase plate 2; turning prisms 3 and 4; lenses 5 and 6; two travelling wave acousto-optical modulators (AOM) 7 and 9 mutually orthogonal, between which lens 8 is mounted; lens 10; mirror 13 with diaphragrams; objectives 11 and 12. On the way of the scattered beam limited by apertures of lenses 11 and 12 and reflected by mirror 13 there are, placed in succession, mirror 14, micro-objective 15, field diaphragm 16 and photodetector 17. The mutually-orthogonal direction of the ultrasonic waves in the modulators corresponds to the orientation of the velocity vector components being measured. The diaphragms of mirror 13 are situated in mutually orthogonal planes and limit the light beams diffracted in the modulators to the zero and minus first order of diffraction, respectively. Phase plate 2 serves to much the polarization of the laser beam with the optical configuration. The photodetector is connected with the two-channel Doppler frequency shift meter

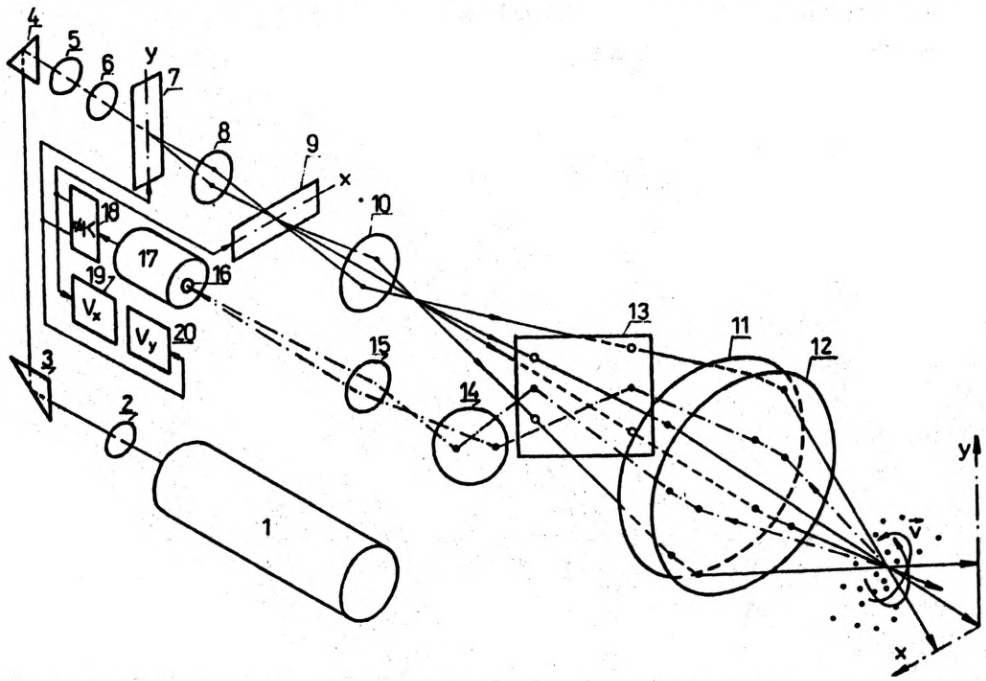

Fig. 1. Optical configuration for LDA with acousto-optical switching of measuring channels (for explation, see text)

involving logic switch 18 connected in parallel with the two Doppler frequency meters 19 and 20, and modulators 7 and 9.

The system functions are as follows. The laser beam after having passed through optical units 2–6, goes to modulator 7. (Propagating ultrasonic wave in the modulator is directed along the Y axis). When modulating voltage is applied to the modulator, two light beams diffracted to the zero and minus first orders are formed at the modulator output operates in the Bragg diffraction mode. Splitted beams go through the train of objective 8, second modulator 9, objective 10, diaphragm 13, objectives 11 and 12, the latter turning them to the flow region under study (i.e., the region with the velocity to be measured). The laser beams intersect and form an interference field with a known periodic structure. The image of this field in the scattered light, limited by field diaphragm 15, is formed by a succession of units 13–16 in the light-sensitive surface of photodetector 17.

When a scattering particle crosses the probe optical field, a radio-pulse appears at the outlet of photodetector. Its frequency is a known linear function of the Doppler frequency shift and its duration is equal to the period required for a scatterer to cross the interference field. The shaper-switch controls modulators 7 and 9 and, after N radio-pulses are applied, connects simultaneously both Doppler frequency shift meters 19 and 20 with photodetector 16. As N decreases, the frequency of information selection increases for each component, reaching its maximum at $N = 2$.

The logic switch comprises a count- and a strobe-pulse shaper. Optical switching of measuring channels is performed at the back front of a strobe-pulse produced by the shaper. Switching takes place when there is no strobe signal and the processor does not store information.

In Figure 2 a functional scheme of acousto-optical switch control is shown. The unit involves shaper of count- and strobe-pulses 1, processors 2 and 3 measuring the V_x and V_y components, modulo N counter 4, digital switch 5, heterodyne 6, mixer 7, photoreceiver 8, high-frequency switch 9, high-frequency amplifiers 10 and 11 connected with the orthogonally-oriented acousto-optical modulator. The system operates as follows. Signal received by photoreceiver 8 (Fig. 2) represents the sum of the Doppler and the carrier frequencies. The latter is determined by heterodyne 6. Mixer 7 operates as a simultaneous detector. At the mixer outlet the Doppler frequency signal is singled out and applied to shaper 1. Output voltage of heterodyne 6 is supplied to high-frequency switch 9 controlled by the output of counter 4. The AOM of the X-channel being switched on, a succession of strobe-pulses is applied to processor 2, while processor 3 is blocked. As the output of counter 4 changes, the X-channel AOM switches off, the Y-channel AOM switches on, processor 2 is blocked and processor 3 operates. Changes in output of counter 4 take place after the N-th input pulse has arrived. Logic level at the counter output changes and switches digital switch enabling the next N pulses of the strobe-pulse sequence to go to the processor. Thus each of the processors, 2 and 3, receives count-pulses only in the course of the strobe-N-pulse sequence. The value of N is usually selected equal to 2. The considered operation algorithm for the logic switch in LDA with adaptive

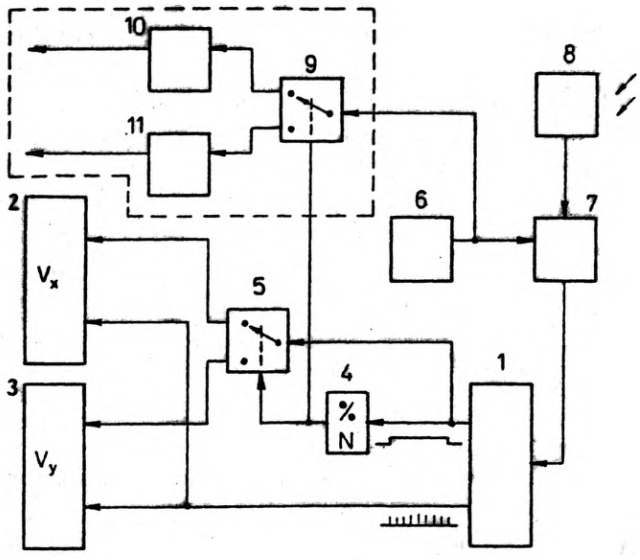

Fig. 2. Acousto-optical switch control (for explanation, see text)

selection of optical signal provides the total laser output used in each measuring channel, which leads to the decrease in relative noise level and improves the measurement accuracy.

Figure 3 demonstrates optical configuration for a meter with electro-optical switch of channels measuring the velocity vector orthogonal components. The meter comprises laser 1 and the following units placed successively on the way of the beam: phase plate 2, lens 3, electro-optical modulator 4, prism 5, phase plates 6, 7 and 8, cubic prism 9. Prisms 10, 11 and 12, phase plates 13 and 14, acousto-optical modulators 15 and 16, lenses 17 and 18, prisms 19, 20 and 21 and objective 22 are placed successively on the way of laser beams splitted by prism 9. Polarization

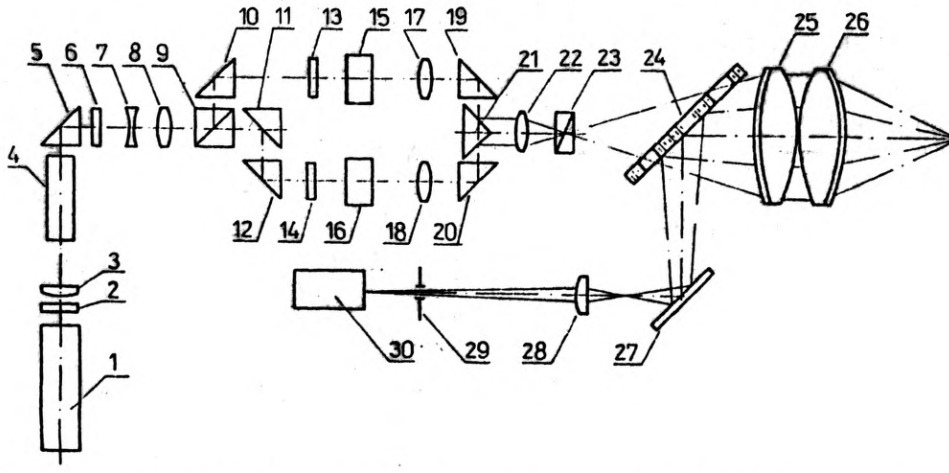

Fig. 3. Optical configuration for LDA with electro-optical switching of measuring channels (for explanation, see text)

Wollaston prism 23 is placed in the intersection area of orthogonally polarized beams. Then the beams, splitted by prism 23, go through the diaphragms of mirror 24 and objectives 25 and 26. Scattered light limited by the above objectives and reflected by mirror 24 comes to the succession of optical units: turning mirror 27, microobjective 28, field diaphragm 29 and at last to photodetector 30 connected to signal processor (refer to Fig. 2). In the configuration described, controlled key 6 switches feed circuit from the half-wave voltage source 7 over to electro-optical modulator in the function of a laser beam polarization switch.

In the measuring configuration of Figure 3, optical train formed by the units with prism 9 at the inlet and prism 21 at the outlet functions as a beam splitter, two parallel orthogonally polarized laser beams with frequency difference specified by accousto-optical modulators 15 and 16 being formed at the outlet. Polarization switch 4 is based on a conversational electro-optical modulator with half-wave voltage control. After passing polarization switch 4 and matching elements 5–8, polarized beam of laser 1 is split by the beam splitter into 2 parallel orthogonally polarized beams with frequency difference corresponding to voltage difference at acousto-optical modulators 15 and 16 operated in Bragg mode. Then the orthogonally polarized beams intersect in the region of polarization Wollaston prism 21. Since the splitting angle of the prism is chosen to the angle between the entering beams, there appear at the prism outlet the orthogonally beams, with polarization being switched on, directed in pairs in orthogonal planes.

Beams emerging from the polarization prism pass objective 25 in pairs, each pair following the other in consecutive order, and form in the investigated medium spatially matched probe interference fields with orthogonal orientation of interference fringes. Additional phase plates may be mounted on the way of beams coming from the prism to match polarizations. Image of the probe interference field in the scattered light is formed at photodetector 30 (photoelectronic multiplier) by objectives 25 and 26, turning mirrors 24 and 27 and microobjective 28, placed in succession. The image formed is confined by field diaphragm 29.

Operation of the signal processor is similar to that in the system with acousto-optical switching of measuring channels. The difference lies in the fact that controlled switch 9 (refer to Fig. 2) switches feed circuit of polarization switch 4 (refer to Fig. 3).

Utilization of the Wollaston prism in this device with traversing of orthogonally polarized light beams at the inlet and splitting angle equal to the angle between the entering beams allows us to change the two-channel structure of conventional devices [3] into a one-channel one. This simplifies significantly the measuring configuration, decreases power loss, makes the adjustment more easy and rises reliability. System with electro-optical switch of polarization enables operation at higher switching frequencies than that with acousto-optical switching.

Laser anemometer is supplied with a pulse-count and a tracking two-channel processors with logic adaptive switching of measuring channels. Maximum switching frequency is 300 kHz. The processor is realized in the CAMAC standard. Operation proceeds in autonomous and computer exchange modes. The device measures two

orthogonal components of the velocity vector and controls particle concentration. Flow of scattering particles causes random discretization of the process. Therefore, the highest frequency of adaptive switching, chosen equal to 300 kHz, allows us to obtain information on velocity fluctuations within a frequency band not exceeding 50 kHz. Let us estimate a potential for frequency measurement accuracy according to the number of zero-crossing of the multi-particle Doppler signal. As is known [4], the average number of zero-crossings for Gaussian process may be determined by

$$\langle n \rangle = \frac{1}{2\pi}\sqrt{-R''(0)} \tag{1}$$

where $R''(0)$ is the second derivative of the correlation function at $\tau = 0$. Assume the Doppler signal is formed by a point scattering particles

$$i(t) = \sum_{i=1}^{N} A(t-t_i)\cos[\Omega(t-t_i)] \tag{2}$$

where $A(t-t_i) = \exp[-\eta(t-t_i)^2]$, ($\eta = \omega_D^2/4\pi^2 M$, ω_D – Doppler frequency shift, $\omega_D = 2\pi V/\Lambda$, Λ – spatial period of the probe optical field); $\Omega = \Omega_0 + \Omega_D$, ($\Omega_0$ – known carrier frequency in measurements with transfer of the Doppler signal spectrum); $2M$ is number of spatial periods in the section of probe optical field. To find the correlation function $R(\tau)$ for the Poisson sequence of radio-pulses (2) we may use the Campbell theorem [4]

$$R(\tau) = \frac{1}{2}\sqrt{\frac{\pi}{2\eta}}\exp\left(-\eta\frac{\tau^2}{2}\right)\left[\exp\left(-\frac{\Omega^2}{2\eta}\right)+\cos\Omega\tau\right].$$

Hence

$$R_0''(0) = \frac{R''(0)}{R(0)} = -\Omega^2\left(1+\frac{\eta}{\Omega^2}\right). \tag{3}$$

Here we took into account that $\exp(-\Omega^2/2\eta) \ll 1$. From (1) and (3) we obtain the average number of signal zero-crossigns

$$\langle n \rangle = \frac{\Omega}{2\pi}\left(1+\frac{\beta^2}{8\pi^2 M^2}\right)$$

where $\beta = \omega_D/\Omega$. Hence, we find relative difference between the average and the actual value of the number of zero-crossings being measured

$$\frac{\Delta\Omega}{\omega_D} = \frac{2\pi\langle n \rangle - \Omega}{\omega_D} = \frac{\beta}{8\pi^2 M^2}. \tag{4}$$

From (4) it is evident that relative difference between the average number of signal zero-crossing and the measured value is in inverse proportion to the square of the number of the probe optical field spatial periods and decreases with increase of carrier frequency Ω_0.

Consider the case when the size of a scattering particle is d. Here the Doppler signal may be presented as a flow of radio-pulses

$$i(t) = \sum_{i=1}^{N} \{A(t-t_i-t_0)\cos[\Omega(t-t_0)-\varphi_0] + A(t-t_i-t_0)\cos[\Omega(t-t_0)+\varphi_0]\}$$

where $t_0 = d/2V = \varphi_0/\omega_D$. By analogy with the previous case we find

$$R_0''(0) = -\Omega^2[1+\frac{\eta}{\Omega^2}-\xi]. \tag{5}$$

The remainder ξ reaches its maximum ξ_m at $2\varphi_0 = (2q+1)\pi$ and $\xi_m = -\beta^2/4\pi^2M^2$. Then, according to (4) and (5),

$$\Delta\Omega/\omega_D = \beta/4\pi^2M^2. \tag{6}$$

This corresponds to the situation when signals from the front and back borders of a scatterer are out-of-phase. In this case the amplitude of the resulting signal is close to zero. A typical experimental Doppler signal illustrating the case is shown in Fig. 4**a**. For comparison, Fig. 4**b** shows a coherent [5] signal obtained by optical

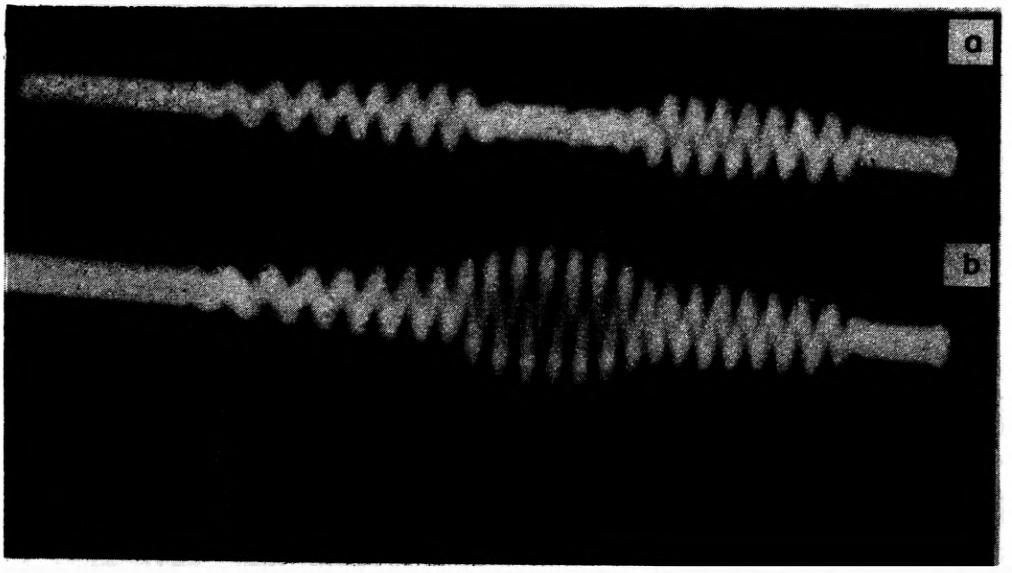

Fig. 4. Incoherent (**a**) and coherent (**b**) Doppler signal from a particle with a size corresponding to the condition

filtration technique. When a particle is of another size, the remainder ξ in (5) is smaller than ξ_m and can be neglected. As follows from (4) and (5), the shifted estimate of the average frequency measured according to the number of signal zero-crossings, may be made by selection of the carrier frequency Ω_0. But the difference between the actual value and the estimate cannot be lower than proper instability of Ω_0. Relative error in determining an average particle appears to be in proportion to β and falls with the increasing Ω_0. This can be accounted to the fact than the increase of Ω_0 leads

to a growing steepness of signal path in zero-cross points and hence to more rigit fixation of zero-crossings.

LDA with adaptive temporal selection of the velocity vector orthogonal components proved its high power efficiency by number of tests. For illustration refer to Fig. 5, where the presented typical Doppler signals are obtained while measuring the fluid flow velocity in backscatter. The distance in water is 0.7 m. A 10 mW He-Ne laser was used as a radiation source. Bandwidth is 2 MHz (Fig. 5**a**) and 100 KHz (Fig. 5**b**). The signal-to-noise ratio is quite sufficient for normal operation of signal processors at even so small a laser power.

Operation in backscatter is featured not only by decreased level of optical signal, but by the effects related to peculiarities of scattering diagram. The latter is cut up by lobes in the angle interval > 90, which leads to a decrease in optical signal contrast

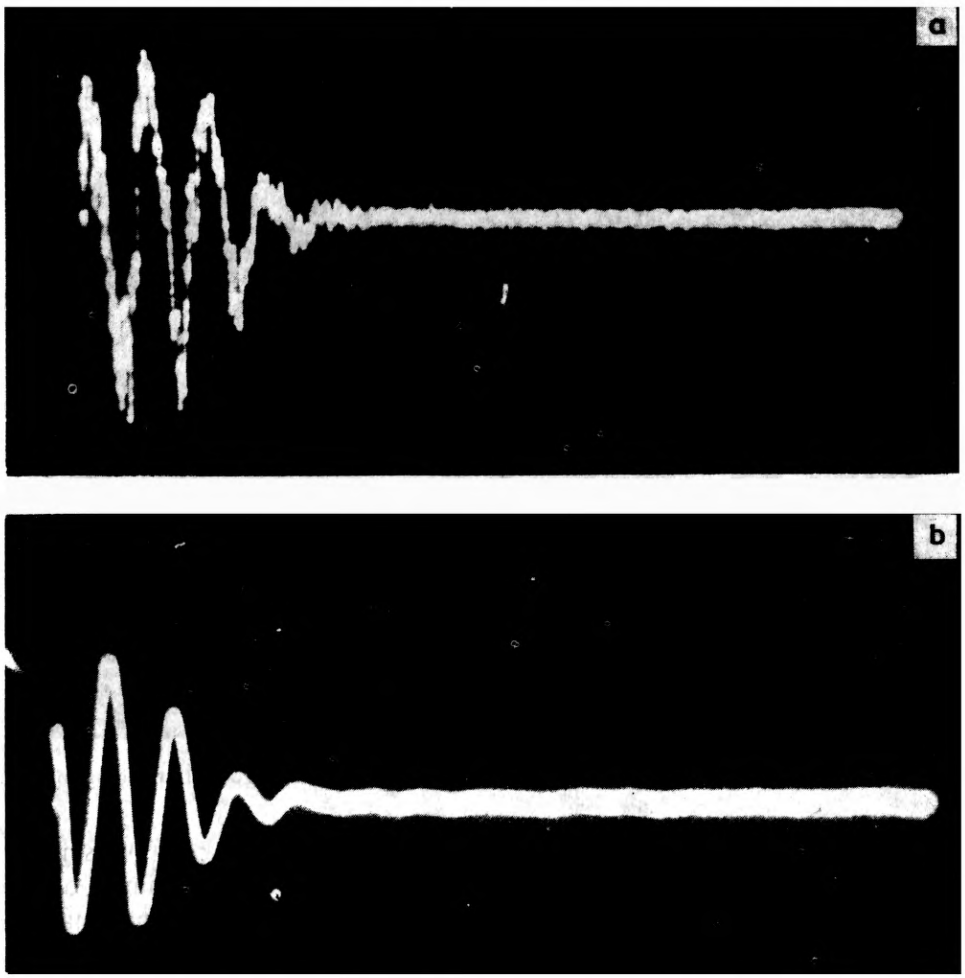

Fig. 5. Doppler signal obtained at flow velocity measurements in backscatter. Distance in water is 0.7 m. Radiation source – He-Ne laser with power output of 10 mW: (**a**) signal in a frequency band of 2 MHz, (**b**) signal in a frequency band of 100 KHz

in measurements using LDA operated in backscatter. This is explained by the fact that coinciding maxima of lobes of the scattering diagram for a particle from two incident light beams forming a probe field occur seldom (maximum signal contrast at mixing scattering waves corresponds to this case). More likely is the situation when ratio of amplitudes of angular spectral components of scattered beams at optical mixing is high, which leads to contrast loss and pedestal in the resulting signal.

When considering the spatial conditions of photomixing, we find that higher amplitude ratio corresponds to larger coherence areas for angular spectral components, and that for spectral components with similar amplitudes the most probable coherence areas are much smaller than the photoreceiver aperture. Therefore, photoelectric signal in backscattering systems looks very different from that in forward scattering ones. The difference lies in the fact that realization of high-contrast radio-pulses occur seldom, while low-contrast with a high pedestal are realized more frequently than in forward scattering case.

Through a scope of experiments we have stated that signal contrast is substantially increased at measurements in backscatter in a wavelength region of the visual radiation range. The increased signal-to-noise ratio in this spectral region is accounted not only to dispersion of the attenuation index with optical radiation propagating in water, but to the properties of a medium as a spatial-frequency filter that influences the structure of optical signal. These properties lead to probe field blurring in scattered light.

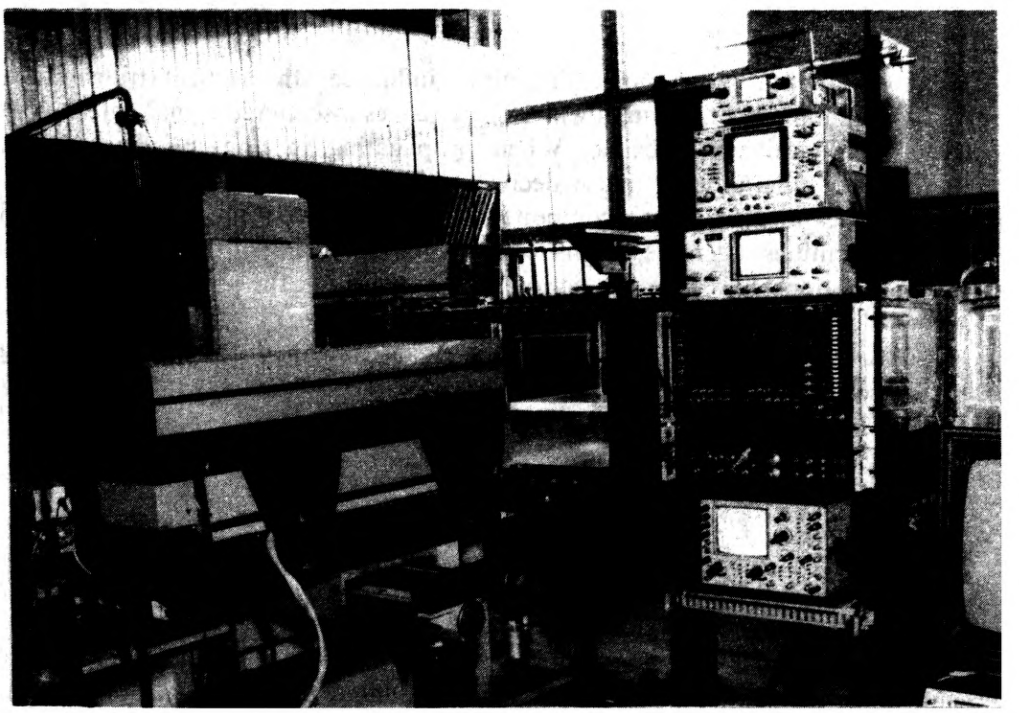

Fig. 6. Photograph of LDA with adaptive temporal selection of the velocity vector orthogonal components

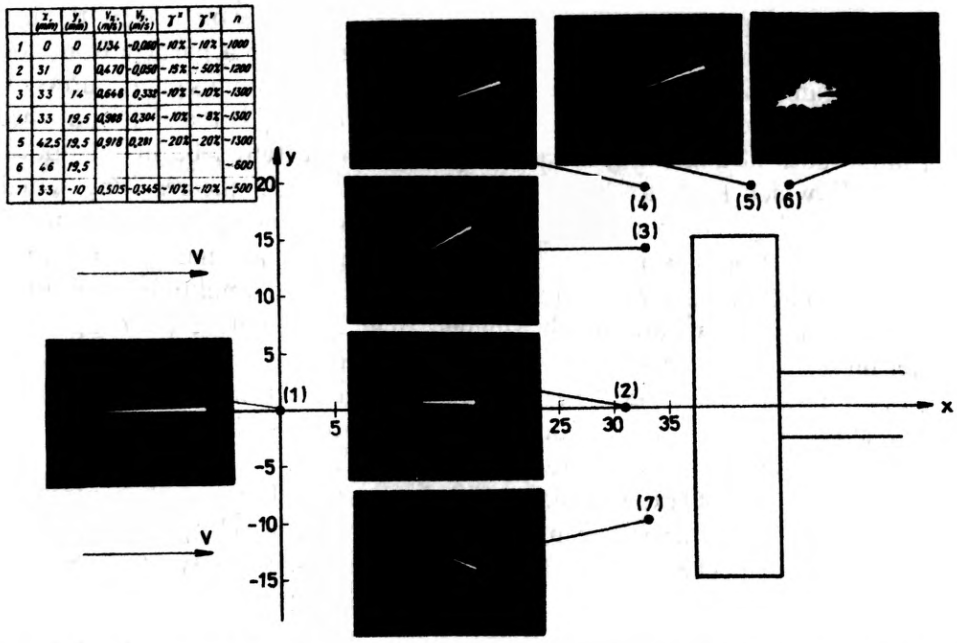

1	0	0	1,134	-0,080	-10%	-10%	-1000
2	31	0	0,470	-0,050	-15%	-50%	-1200
3	33	14	0,646	0,330	-10%	-10%	-1300
4	33	19,5	0,908	0,304	-10%	-8%	-1500
5	42,5	19,5	0,918	0,281	-20%	-20%	-1300
6	46	19,5					-600
7	33	-10	0,505	-0,345	-10%	-10%	-500

•Fig. 7. Visualized velocity vector in different points of liquid flow around a disc body in points 1–7: X and Y – coordinates of the point; V_x and V_y – X and Y velocity components; γ^x, γ^y – turbulent intensity; n – count of particles intersecting the probe volume (in s)

Field of random phase non-uniformities influences the optical transmission function of medium layer, through which there passes a scattered signal entering the aperture of a receiving objective. When propagating in non-uniform medium, fluctuations of a light beam phase decrease as the wavelength increases. Liquid medium filtrates high-frequency components of angular spectrum of optical signal. As non-uniformities decrease, high-frequency components of angular spectrum become more suppressed. The rise in power flow density in the probe field and laser radiation selected with a large wavelength lead to the increase of contrast and level optical signal. Fig. 6 shows the laser anemometer near hydrodynamic tube. Fig. 7 shows photographs of the visualized velocity vector in different points of liquid flow around a disc body.

3. Conclusions

Laser Doppler anemometers with adaptive temporal selection of the velocity vector are featured by the high power efficiency. This is due to the fact that the total laser power is used to measure one velocity component. Communication noise and interaction of measuring channels are excluded, since switching takes place during such intervals when there are no Doppler radio-pulses. Switching frequency is determined by scattering particle distribution and dynamics of the process under investigation.

Relative easiness of realization, compatibility with conventional optical configurations and signal processing systems, are the advantages making the method of adaptive temporal selection of the velocity vector in LDA deserving consideration and development.

References

[1] DURST F., MELLING A., WHITELAW J. H., *Principles and Practice of Laser-Doppler Anemometry*, Academic Press, London 1976, p. 295.
[2] DUBNISTCHEV Yu. N., RINKEVITCHUS B. S., *Metody lazernoi doplerovskoi anemometrii*, (in Russian), Nauka, Moskva 1982, p. 164.
[3] BAHNEN R. H., KOELLER K. H., Rev. Sci. Instrum. **55** (1984), 80–83.
[4] TIKHONOV V. I., *Statisticheskaya radiotekhnika* (in Russian), Sovetskoe Radio, Moskva 1966, p. 678.
[5] DRAIN L. E., Appl. Phys. **5** (1972), 481–483.

Received June 22, 1989
in revised form May 22, 1990

Лазерный доплеровский анемометр с адаптивной временной селекцией вектора скорости

В работе описывается лазерный доплеровский анемометр с адаптивной селекцией и визуализацией вектора скорости. Логическая коммутация измерительных каналов, определяющих две ортогональные компонетны вектора скорости, соответствует пространственному распределению и динамике рассеивающих частиц в потоке. В приборе реализован синтезатор изображения вектора скорости в реальном времени. Метод адаптивной временной селекции вектора скорости отличается высокой энергетической эффективностью и помехоустойчивостью за счет исключения коммутационных шумов.